Senge, M. O.; Flanagan, K. J.; Ryan, A. A.; Ryppa, C.; Donath, M.; Twamley, B. (2016):
Conformational and Structural Studies of meso Monosubstituted Metalloporphyrins – Edge-on molecular interactions of porphyrins in crystals.
Tetrahedron 72, 105–115. doi: 10.1016/j.tet.2015.11.008

Graphical Abstract

Conformational and structural studies of meso monosubstituted metalloporphyrins – Edge-on molecular interactions of porphyrins in crystals

Mathias O. Senge, Keith J. Flanagan, Aoife A. Ryan, Claudia Ryppa, Mandy Donath, and Brendan Twamley
School of Chemistry, Trinity College Dublin, the University of Dublin, Dublin, Ireland

Leave this area blank for abstract info.

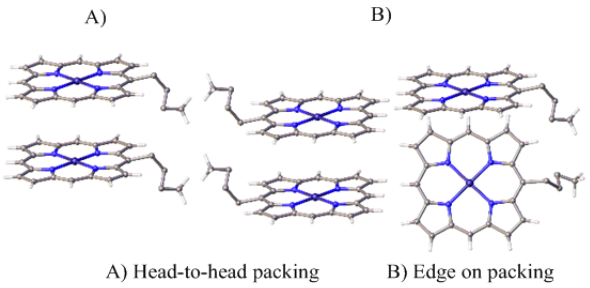

Conformational and Structural Studies of meso Monosubstituted Metalloporphyrins – Edge-on molecular interactions of porphyrins in crystals

Mathias O. Senge,[a,*] Keith J. Flanagan,[a] Aoife A. Ryan,[a] Claudia Ryppa,[b] Mandy Donath[b] and Brendan Twamley[a]

[a] School of Chemistry, SFI Tetrapyrrole Laboratory, Trinity Biomedical Sciences Institute, 152-160 Pearse Street, Trinity College Dublin, The University of Dublin, Dublin 2, Ireland
[b] Institut für Chemie, Universität Potsdam, Karl-Liebknecht-Str. 24-25, 14476 Golm, Germany

∗ Corresponding author. Tel.: +353-1-896-8537; fax: +353-1-896-8536; e-mail: sengem@tcd.ie

A series of meso monosubstituted metalloporphyrins were synthesized to assess the structural chemistry of porphyrins with only one substituent. The structures of four nickel(II) and zinc(II) complexes with either alkyl or aryl residues indicate primarily planar macrocycles. This gives rise to a different type of π-interactions in the crystal and the formation of dimeric, trimeric or tetrameric porphyrin units that function as building blocks for the overall crystal structure. Notably, some structures exhibit a unique edge-on packing of porphyrins, while the molecules of (5-*n*-butylporphyrinato)nickel(II) forms an unusual bilayer type structure where rows of two porphyrin macrocycles are separated by the alkyl residues arranged in a head-to-head fashion. This adds to the canon of intermolecular porphyrin packing arrangements and is of relevance for the preparation of ordered nanoscopic porphyrin devices.

Key words: Porphyrins; Conformational Analysis; Tetrapyrroles; Crystal Structure; Crystal Packing

1. Introduction

Porphyrins are often described as the prime examples of macrocycles capable of coordinating almost any metal in the core. This and their binding by apoproteins are then taken as a basic rationale for their biological function at a molecular level. Further fine-tuning is achieved through the type of central metal and its axial ligation.[1] Additionally, the peripheral substituents modulate the porphyrin properties through electronic and conformational effects. Numerous studies have been performed on these conformational substituent effects, mainly investigated with highly substituted porphyrins, *e.g.*, dodecasubstituted, nonplanar porphyrins, where a large number of residues resulted in steric congestion at the macrocycle periphery with attendant changes in structural and physicochemical properties.[2]

At the other end of the spectrum are porphyrins with as few substituents as possible.[3] Only recently have advances in synthetic methodology made an entry in this field possible.[4,5,6,7,8] A typical example is the so-called A_x-series of porphyrins (**1**-**6**, Fig. 1), where 0–4 meso substituents allow a detailed comparison of the electronic and structural effects of macrocycle substitution. In terms of physical characterization this has given rise to studies on the interrelationship of substituents and redox potential and, in materials chemistry, on the influence of the number and regiochemistry of meso substituents on the type and formation of differently sized nanospheres and nanorods.[9] They also allow the preparation of more unsymmetrical systems, *e.g.*, the ABCD-type porphyrins,[5,10] and studies on the effect of mixed types of substitution. While porphyrins with four (**6**) and two substituents in a 5,15-pattern (**3**) constitute materials widely used in porphyrin chemistry, the mono- (**2**) and 5,10-disubstituted (**4**) are only now beginning to be used in synthetic applications.[4,6]

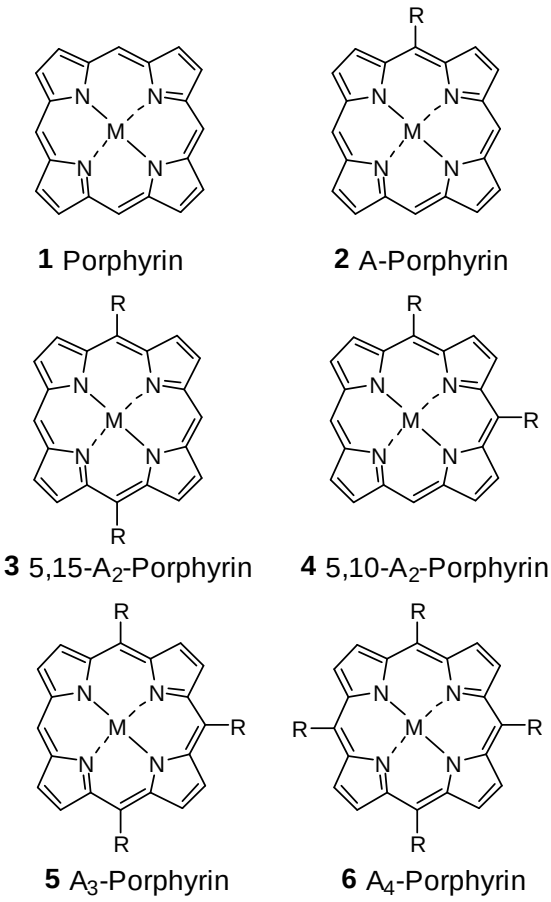

Figure 1. The A_x-porphyrin series.

With regard to structural chemistry, past studies have compared the 5,15-A_2- and 5,10-A_2 regioisomers,[8,11] and the influence of individual bulky meso substituents.[12] However, structural data are still scarce for meso monosubstituted porphyrins. Here we present the results of X-ray crystallographic studies on 5-substituted metalloporphyrins and aim to elucidate some key aspects and general trends of their structural chemistry identifying a unique type of intermolecular interactions for porphyrins. We are also presenting the first crystal structures of 5-substituted Zn(II) porphyrins and add to existing structures of 5-substituted Ni(II) porphyrin structures.[12a]

2. Results and Discussion

Metal complexes of the $A_{\text{-type}}$ free base porphyrins were prepared using standard reaction conditions[13,14] and used for crystallization attempts. In addition, a few 5,15-A_2 metalloporphyrins were prepared as well. Within a given series, *i.e.* 5- or 5,15-disubstitution, their spectroscopic characteristics follow the trends observed for the related A_4 porphyrins.[15] For example, for the A-series **Ni(II)2** the meso arylporphyrins exhibit Soret and long wavelength absorption bands at ~392 and 541 nm, while the primary and secondary alkylporphyrins show only a negligible shift of these absorption bands to 394 and 543 nm. However, the *t*Bu derivative **Ni(II)2c** has significantly bathochromically shifted absorption bands at 404 and 567 nm, which is indicative for a distorted macrocycle in solution.[12]

Despite many attempts over 12 years, only four of the monosubstituted metalloporphyrins yielded crystals of sufficient quality for single crystal X-ray crystallographic investigations. The structures obtained are those of **Ni(II)2a**, **Zn(II)2e**, **Zn(II)2f**, and **Ni(II)2h**. Figure 2 gives thermal ellipsoid view of the molecular structures of the porphyrins.

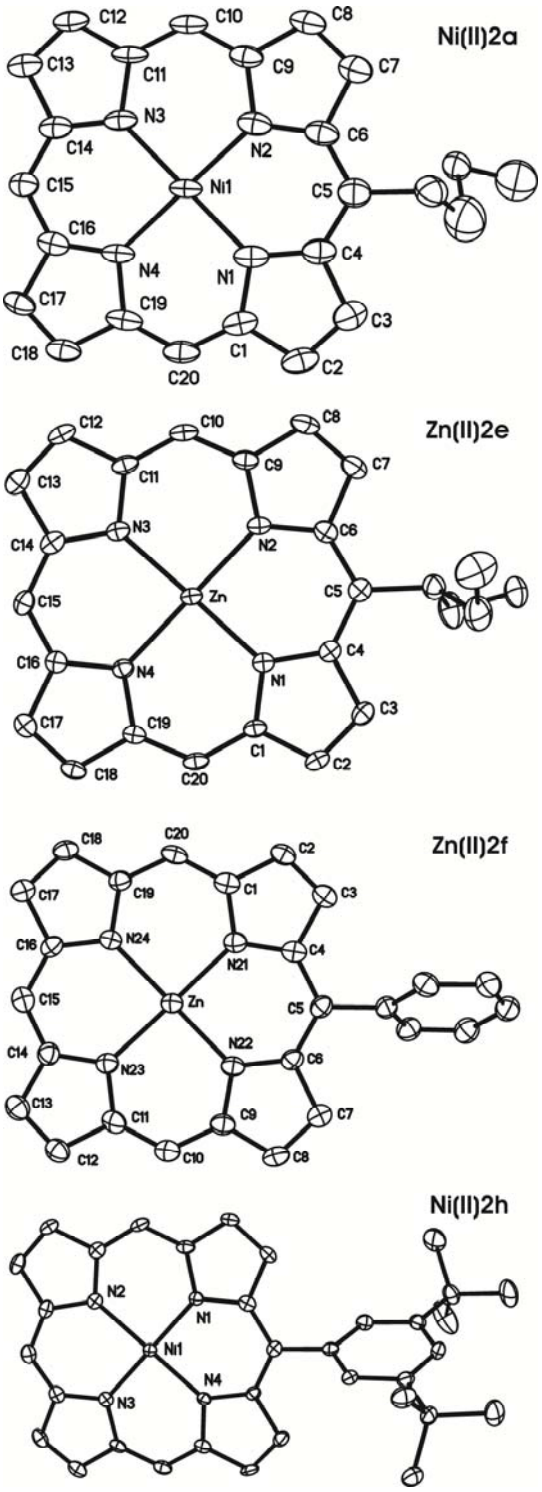

Figure 2. View of the molecular structures of the compounds studied in the crystal. Thermal ellipsoids show 50 % probability. Hydrogen atoms and disordered positions have been omitted for clarity. Only one of the crystallographically independent molecules is shown for **Zn(II)2f** and **Ni(II)h**.

At first glance the structure of **Ni(II)2a** is that of a standard porphyrin. The average Ni-N bond length of 1.951(10) Å agrees will that of the respective A_4-porphyrin **Ni(II)6a** [1.943(1) Å].[15c] In line with earlier observations on meso monosubstituted 2,3,7,8,12,13,17,18-octaalkylporphyrins,[16] the C_a-C_m-C_a bond angle for the substituted meso position is smaller [120.6(5)º] than the one of the unsubstituted positions (average bond angle = 123.8(5)º). Rough structural parameters, such as the average deviation of the 24 macrocycle atoms from their least-squares plane (Δ24) show the porphyrin to be planar and the C_m positions show no evidence for localized displacements (Table 1). Ni(II)porphyrins which present less substituted meso-porphyrins often show no core contraction. Kozlowski *et al.* suggested that Ni(II)porphyrins occupy a d^8 singlet conformation resulting in eight electrons being doubly occupied manifold d-orbitals leaving the $d_{x^2-y^2}$ empty.[17] This results in a small core size in Ni(II)porphyrins. Both removal, creating of a low spin, and addition, occupying higher d-orbitals, of an electron results in an increase in the size of the metal core. As substitutions are made to the porphyrin macrocycle, electron density can be either contributed or removed from the ring resulting in changes to the contractions of the Ni(II) core. There are short contacts between the pyrrole ring and β-hydrogen atoms on neighboring units in the range of 2.6-2.8 Å are present in the packing of the unit cell. However no interaction with the core seems to be present.

However, the crystal packing is unlike anything that we have ever seen in substituted porphyrins (Fig. 3). Despite the short alkyl chain, the porphyrin forms parallel running arrays with the alkyl chains pointing towards each other and two porphyrin macrocycles forming the other side of the chains; a situation reminiscent of the lipid-bilayer membranes in nature. There is no evidence of π-interactions or aggregate formation in the crystal. The 4N-planes of neighboring molecules within a row of porphyrins are tilted against each other by 64.4º (Fig. 4). The C_b and C_m hydrogen atoms on one molecule point towards the edge of a neighboring molecule. In fact, the packing is rather tight; *e.g.*, the C_m-H in one molecule is only separated by 2.97 Å from the C_m atom in the next molecule.

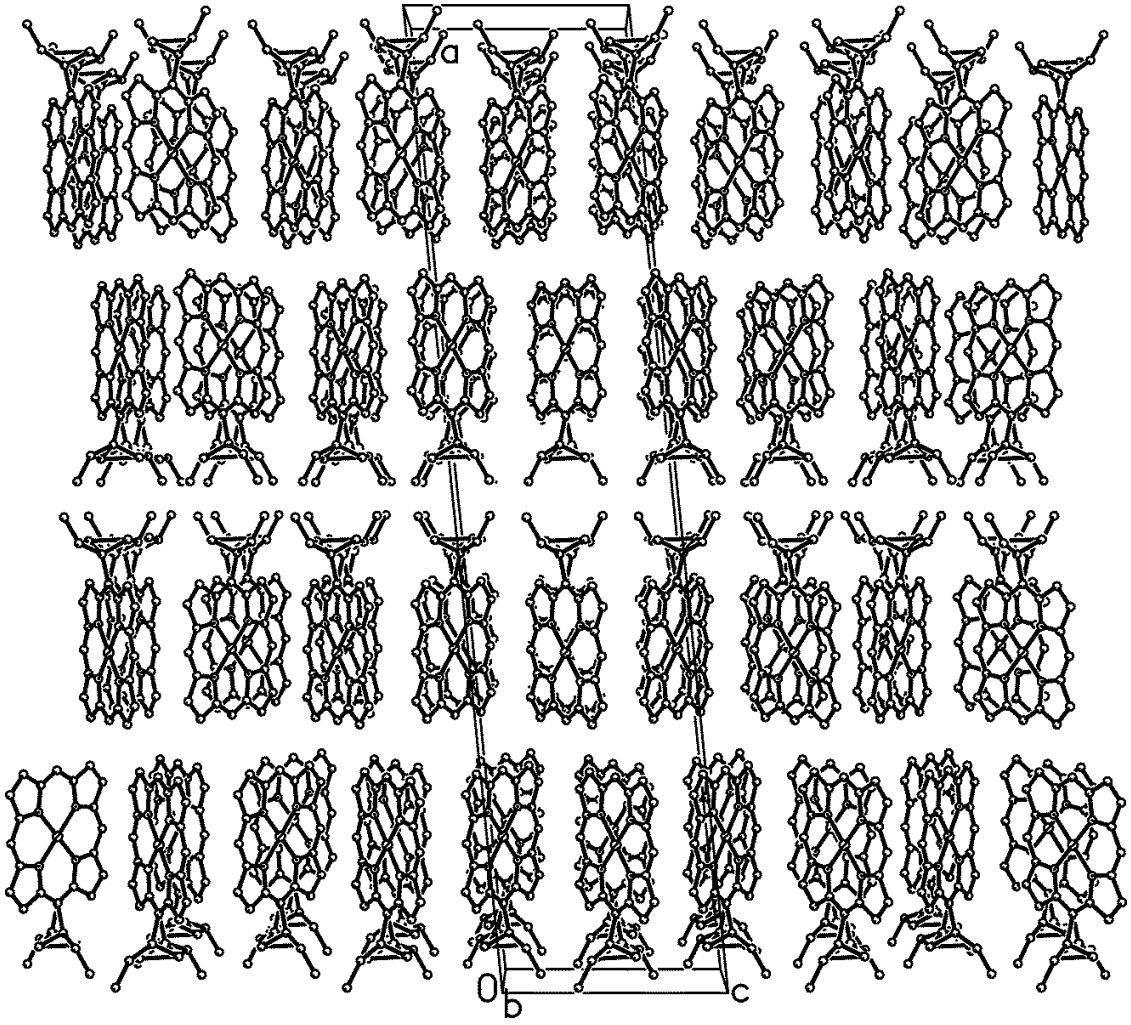

Figure 3. View of the molecular arrangement in the crystal of **Ni(II)2a** (down b-axis). Hydrogen atoms have been omitted for clarity. Note, both disordered positions of the *n*-butyl residues are shown to illustrate the overall "space-filling" effect.

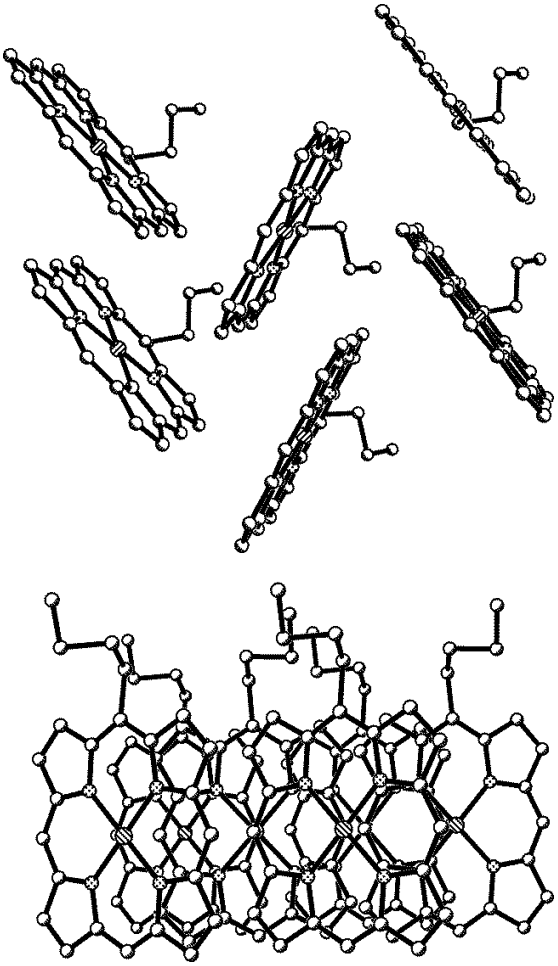

Figure 4. Side (top) and top (bottom) view of one of the porphyrin layers in the crystal structure of **Ni(II)2a** (down b-axis). Hydrogen atoms and disordered positions have been omitted for clarity.

The crystals of **Ni(II)2e** (space group *C2/c*, a = 50.84, b = 6.49, c = 11.63 Å, β = 90.95º, data not shown due to low resolution) are isomorphous to that of **Ni(II)2a**. Thus, exchange of a meso *n*-butyl chain for an 1-ethylpropyl residue does not alter the overall molecular arrangement or the conformational aspects.

Similarly, the structure of **Zn(II)2e** exhibits a planar macrocycle with Δ24 = 0.028 Å and a smaller C_a-C_m-C_a bond angle for the substituted meso position (123.8º *versus* an average of 126.9º for the unsubstituted ones). The zinc center is tetracoordinated with an average Zn-N bond length of 2.047(2) Å similar to that of **Zn(II)6f** 2.043(5) Å.[18] The molecular packing (Fig. 5) is characterized by the formation of standard head-to-tail dimeric aggregates.[19] According to the classification given by Scheidt and Lee[1] the dimers are characterized by a center-to-center (Ct–Ct) distance of 5.114 Å, a mean-plane separation (MPS) of 3.07 Å and a slip angle (SA) of 53.1º. This give rise to a lateral shift (LS = [sin (SA) × Ct–Ct]) of 4.08 Å, which puts this structure into the "I" (intermediate)[1] category.

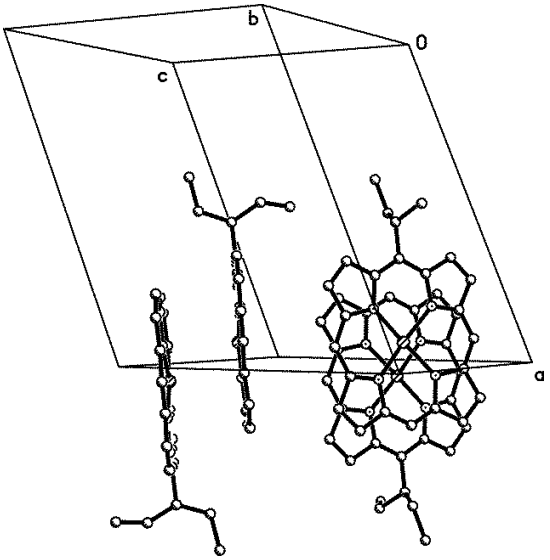

Figure 5. View of the π-aggregates formed in the crystal of **Zn(II)2e**. Hydrogen atoms have been omitted for clarity.

The relatively close mean-plane separation, as defined by the separation of the two 4N-planes, also gives results in short intermolecular contacts. Thus, the two neighboring zinc centers are separated by only 3.522 Å and each zinc center is "coordinated" by N4 from a neighboring molecule with a separation of 2.95 Å. As shown in Figure 5 neighboring dimers are orthogonal to each other with a close contact of 3.08 Å between Zn and H18A. The dimeric unit shows many close contacts, around 3.35 Å, between both porphyrin rings which stabilize the head-to-tail arrangement in the packing order. Other close contacts present are between β hydrogen atoms of one dimer and the nearest molecular unit with a distance of 2.35-2.84 Å. The final close contact is between H55a and H17a of the nearest molecular unit with a distance of 2.545 Å. Overall, these units of two dimers are arranged in parallel layers with the porphyrin macrocycle in the middle and the alkyl chains pointing outwards (not shown).

Compound **Zn(II)2f** formed crystals with three crystallographically independent porphyrins in the asymmetric unit. The core geometry about the zinc(II) centers is similar to that of other planar zinc(II) porphyrins with a tetracoordinated metal center. The average Zn-N bond length of 2.038 Å. This is comparable with earlier work conducted within the group on meso tetrasubstituted porphyrin Zn(II) complexes **Zn(II)6c (**2.014 Å) and (5,10,15,20-tetracyclohexylporphyrinato)zinc(II) (2.029 Å).[15c] The three macrocycles are planar, although minor C_m displacements are observed. Substitution of the 5-position with an aryl residue results in much smaller differences in the C_a-C_m-C_a bond angles compared to the alkylporphyrins. The porphyrins are arranged in layers with the meso phenyl groups pointing outwards (not shown). This is the result of an unusual head-to-tail trimer formation in the crystal. Figure 6 illustrates how these units of three porphyrins function as the building blocks within one of the layers in the crystal.

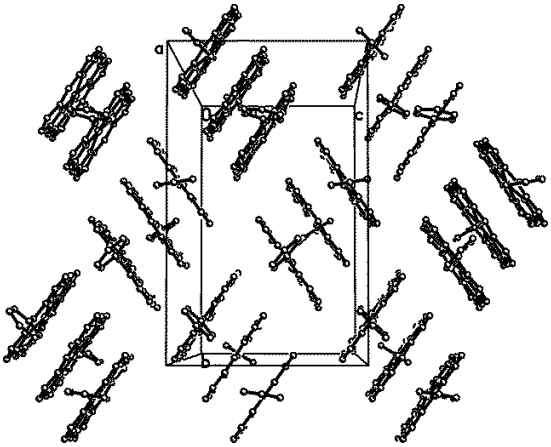

Figure 6. View of the trimeric π-aggregates formed in the crystal of **Zn(II)2f**. Hydrogen atoms have been omitted for clarity.

These trimeric units are held together by relatively strong π-π-interactions. With three zinc centers (ZnB is sandwiched between Zn and ZnA) present the geometry of these units can be described as follows: The Ct–Ct distance between Zn and ZnB is 3.679 Å, with a mean-plane separation of 3.139 Å and a slip angle of 31.5º. For the two macrocycles comprised of ZnB and ZnA the related values are 3.663 Å, 3.133 Å and 31.2º, respectively. Thus the lateral shifts of the centers are 1.922 Å for Zn…ZnB and 1.898 Å for ZnB…ZnA. This puts these π-interactions at the upper end of the S (strong) category defined by Scheidt and Lee.[1]

The structure of the nickel(II) complex of 3,5-di-*tert*-butylporphyrin **Ni(II)2h** contains four crystallographically independent porphyrins in the asymmetric unit. All show minor to significant degrees of nonplanarity with Δ24 values ranging from 0.08 to 0.18 Å. The main deviations from planarity involve the C_m positions which are alternatively displaced above and below the 4N-plane. The Ni- bond length range from 1.94 to 1.96 Å which is similar to those observed in **Ni(II)2a**. With regards to higher substituted Ni(II) complexes the bond lengths are marginally smaller in **Ni(II)6f** (1.931 Å) and (5,10,15,20-tetra(*iso*-butyl)porphyrinato)nickel(II) (1.909(3) Å).[15c] The C_a-C_m-C_a bond angles show a similar trend as observed in the other structures reported here, with the substituted position exhibiting a smaller angle. However, the difference between substituted and unsubstituted positions is somewhat smaller than observed in (5,15-diisopropylporphyrinato)nickel(II) (119º for the substituted position and 124º for the unsubstituted position).[20]

The molecular packing of **Ni(II)2h** is characterized by the formation of rows of porphyrin arrays which are separated by the meso substituents (Fig. 7). Chloroform molecules of solvation are located in the void between the porphyrin rows. The four porphyrins in the asymmetric unit are grouped in two pairs of π-aggregated dimers which serve as the building blocks of the overall structure in the crystal (Fig. 8). One dimer (Ni3, Ni4) is of the standard head-to-tail type and pertaining geometric parameters are MPS = 3.415 Å, Ct–Ct = 4.174 Å, SA = 45.1º giving a lateral shift of the metal centers of

2.95 Å. Intriguingly, the other 'dimer' (Ni1, Ni2) is of the head-to-head type with both meso residues pointing in the same direction. Here the two macrocycles are separated by 3.37 Å (MPS), have a Ct–Ct distance of 4.196 Å and a SA of 36.5 Å, resulting in a LS of 2.496 Å. Thus, despite the sterically more unfavorable head-to-head arrangement this aggregate is stronger than the head-to-tail one. A number of close intermolecular contacts were observed as well [Ni2-H114 3.135 Å, N9-H10 2.609 Å, N13-H10 3.144 Å, Ni1-H46 3.055 Å, C120-H82 2.767 Å, C108-H78 2.715 Å].

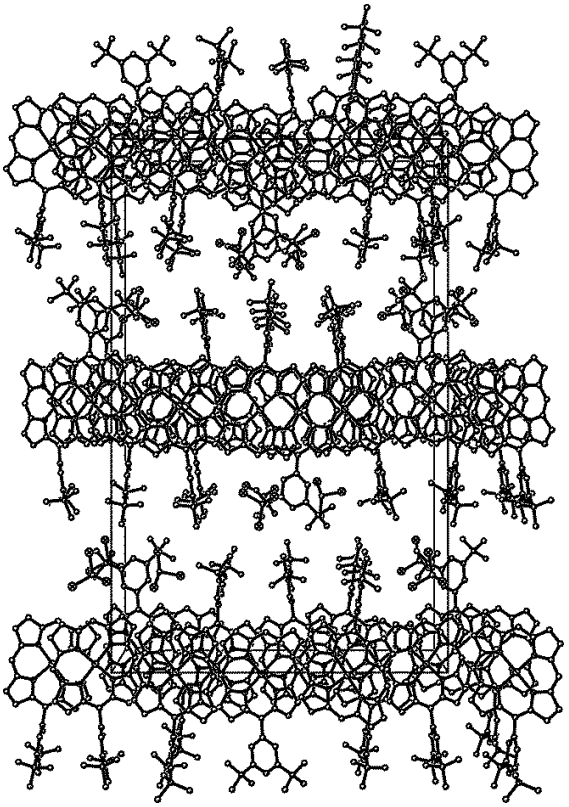

Figure 7. Side (top) and top (bottom) view of one of the porphyrin layers in the crystal structure of **Ni(II)2h** (down a-axis). Hydrogen atoms and disordered positions have been omitted for clarity.

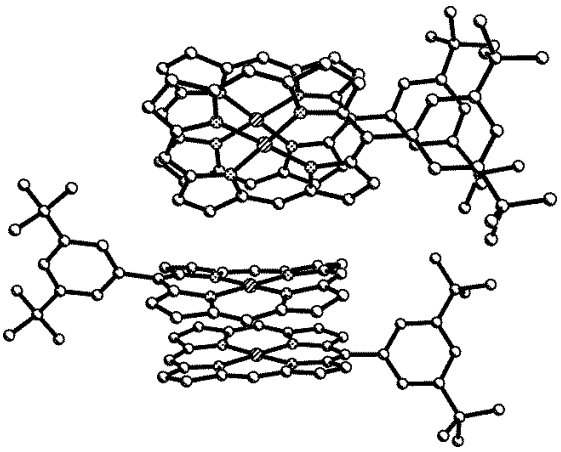

Figure 8. View of the four molecules of **Ni(II)2h** in the asymmetric unit. Hydrogen atoms and disordered positions have been omitted for clarity.

In comparison the two available structures for metal complexes of mono-*tert*-butylporphyrin exhibit more typical π-stacked aggregates.[21] In the nickel(II) derivative **Ni(II)2c**, with one crystallographically independent molecule in the asymmetric unit, four 'dimers' fill the unit cell with the meso substituents offset by 90º against each other.[12a] The copper(II) derivative **Cu(II)2c** exhibits the standard head-to-tail formation of I-type aggregates.[12b] Here, the asymmetric unit contains two crystallographically independent molecules, which form π-aggregates, which in turn themselves form π-aggregates of I-type. Thus, here four porphyrin units form the main building blocks in the crystal.

All structures determined here exhibit a significant number of short non-bonding interactions and close contacts within the individual packing arrangements. *E.g.*, compound **Ni(II)2a** presents with the majority of its short contacts being interactions between the β-hydrogen atoms and the pyrrole rings at a distance of 2.89-2.29 Å. **Zn(II)2e** exhibits similar contacts with separations of 2.84-2.64 Å, **Zn(II)2f** shows contact distances of 2.88-2.66 Å and in **Ni(II)2h** there are interactions with a pyrrole ring of a neighboring macrocycle of 2.7-2.8 Å. β-Hydrogen atoms can also be seen to interact with solvent chloroform molecules in **Ni(II)2h** with contacts distances of 2.94-2.87 Å. The 5-meso substituted unit also participates in short contacts within the crystal structure. For example, in **Ni(II)2a** close contacts between the butyl substituents in neighboring molecules are in the order of ~2.7 Å.

A rough inspection of the macrocycle structures using displacement parameters (Table 1) indicates that most of the 5-R-metalloporphyrins have a planar macrocycle. Only when the sterically highly demanding *tert*-butyl group is introduced do large deviations from planarity occur.[12] However, the presence of multiple porphyrins within some asymmetric units and the different packing arrangements prompted us to analyze the macrocycle conformations in more detail. This can only be done by the normal-structural decomposition which allows an identification and comparative analysis of individual distortions modes.[22] Figure 9 details the results for an analysis of all available **M2** structures.

Table 1. Selected structural parameters and conformational descriptors for 5-substituted metalloporphyrins [Å, °].

	Ni(II)2a	**Zn(II)2e**	**Zn(II)2f**			**Ni(II)2h**				**Ni(II)2c**[12a]	**Cu(II)2c**[12b]	
			M1	M2	M3	M1	M2	M3	M4		M1	M2
Ct-$N_{av.}$ [a]	1.952	2.037	2.035	2.035	2.037	1.954	1.948	1.940	1.955	1.902	1.988	1.985
M-N21	1.942(4)	2.029(2)	2.038(5)	2.035(6)	2.022(5)	1.950(3)	1.946(3)	1.939(3)	1.958(3)	1.906(6)	1.908(3)	1.983(3)
M-N22	1.948(5)	2.041(2)	2.039(6)	2.034(5)	2.033(6)	1.961(3)	1.951(3)	1.942(3)	1.953(3)	1.893(6)	1.984(3)	1.983(4)
M-N23	1.961(4)	2.036(2)	2.038(6)	2.052(6)	2.041(6)	1.951(3)	1.948(3)	1.935(3)	1.962(3)	1.900(6)	1.988(3)	1.988(4)
M-N24	1.958(4)	2.058(2)	2.044(5)	2.031(5)	2.051(6)	1.953(3)	1.948(3)	1.943(3)	1.945(3)	1.905(6)	2.000(3)	1.988(3)
C4-C5-C6	120.6(5)	123.8(2)	125.0(6)	125.8(6)	125.2(6)	122.3(4)	122.2(4)	121.7(4)	122.0(4)	119.3(7)	119.6(3)	119.2(4)
C9-C10-C11	123.8(5)	127.3(2)	126.5(6)	125.5(6)	126.5(6)	124.6(4)	124.1(4)	123.7(4)	124.4(4)	123.3(7)	125.7(4)	126.5(4)
C14-C15-C16	123.1(5)	126.5(3)	126.4(6)	126.6(7)	127.2(6)	124.1(4)	123.2(4)	123.2(4)	122.8(4)	122.4(7)	125.4(4)	125.9(4)
C19-C20-C1	124.6(6)	126.9(2)	125.8(6)	126.8(6)	126.9(6)	124.0(4)	124.2(4)	123.9(4)	123.6(4)	122.5(7)	126.3(4)	126.3(4)
D_{oop} [b]	0.0402	0.1627	0.1934	0.2035	0.1667	0.4725	0.5341	0.9994	0.5408	2.023	1.16	1.1624
D_{ip} [c]	0.1455	0.1948	0.1478	0.1433	0.1441	0.1568	0.1742	0.2404	0.1649	0.572	0.1939	0.2061
Θ [d]	0.044	0.062	0.03	0.004	0.02	0.03	0.03	0.03	0.05	0.068	0.051	0.073
Δ24 [e]	0.007	0.028	0.036	0.03	0.03	0.084	0.092	0.175	0.093	0.34	0.197	0.195
δC5 [f]	-0.01	-0.06	-0.07	0.05	0.01	0.15	-0.2	-0.38	0.09	0.88	0.60	0.63
δC10 [f]	-0.01	0.1	0.02	-0.11	0.13	-0.18	0.2	0.21	-0.21	-0.68	-0.28	-0.34
δC15 [f]	-0.01	0.1	0.07	-0.10	0.01	0.15	-0.14	-0.33	0.14	0.63	0.21	0.26
δC20 [f]	0.02	0.01	0.06	-0.04	-0.13	-0.18	0.21	0.31	-0.17	-0.67	-0.30	-0.33

[a] core size; [b] simulated total out-of-plane distortion; [b] simulated total in-plane distortion; [d] core elongation parameter = difference in N•••N vector lengths: [(N21—N24) + (N22—N23)] – [(N21—N22) + (N23—N24)]; [e] average deviation from the least-squares plane of the 24-macrocycle atoms; [f] displacement of the atom from the 4N-plane.

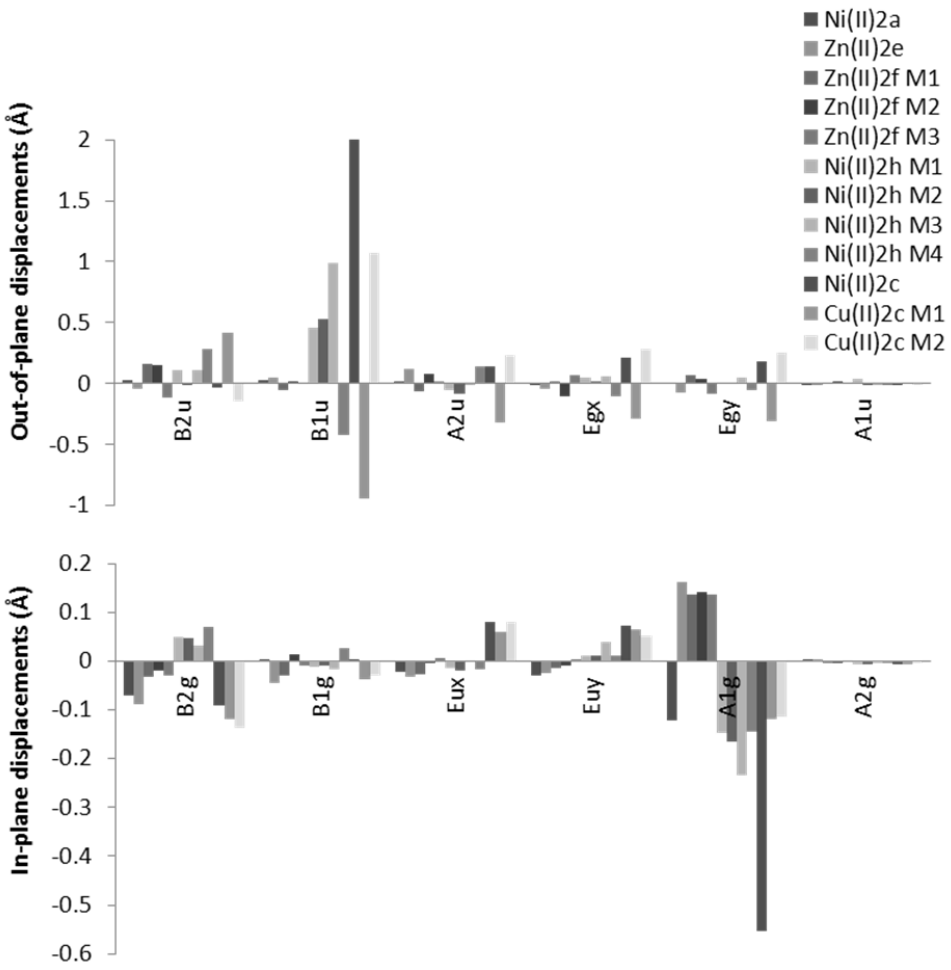

Figure 9. Normal-coordinate structural decomposition analysis of 5-substituted metalloporphyrins (minimal basis).

For the out-of-plane distortions significant contributions are observed for the *ruf* (B_{1u}) and *sad* (B_{2u}) distortions modes, with minor contributions from doming (A_{2u}) and wave (E_g) distortions. No measurable contribution for *pro*pellering (A_{1u}) was observed in any compound. In terms of in-plane distortions a similar picture emerges. Here, strong A_{1g} (*bre*athing), medium B_{2g} (*m*eso-*str*), minor *N-str* (B_{1g}) and noticeable E_u (*pyr-tr*anslations), albeit no *pyr-ro*tation (A_{2g}), were found. Clearly the substituent pattern, *i.e.* A-type (**2**), gives rise to a unique mix of distortion modes. Overall, significant in-plane distortions are present, although not strong enough to give rise to a significant core-elongation. As expected the *tert*-butyl derivatives exhibit the largest contributions from each individual distortion mode, an indication of the steric strain imposed by the bulky residue. Still, **Ni(II)2h** exhibits a considerable contribution from *ruf* distortion, too, larger than the other sterically unhindered derivatives. However, overall the two Ni(II)porphyrin structures reported here show core-geometries similar to triclinic (2,3,7,8,12,13,17,18-

octaethylporphyrinato)nickel(II) and (5,10,15,20-tetramethylporphyrinato)nickel(II), which are planar.[23] Significant ruffling becomes apparent only with secondary alkyl substituents, *e.g.*, as indicated by the shorter average Ni-N bond length of 1.907(7) Å in **Ni(II)4b**.[15c]

3. Conclusions

In conclusion, four new meso monosubstituted metalloporphyrins structures were investigated with X-ray diffraction. Typically substituted metalloporphyrins form head-to-tail type π-aggregates.[1,19] Without meso substituents these aggregates can be quite strong and, as shown, can present a unique packing arrangement depending on the substituents involved. Within the four structures presented the 'blocking' of one side of the tetrapyrrole ring leaves three sides to participate in tighter packing arrangements (*e.g.*, **Zn(II)2e**, **Zn(II)2f** and **Ni(II)2h**) or novel crystal packing motives as seen in **Ni(II)2a**. We have also shown the first two examples of crystals structures of 5-substituted Zn(II) porphyrins (**Zn(II)2e** and **Zn(II)2f**) and added two new structure of 5-substituted Ni(II) porphyrins (**Ni(II)2h** and **Ni(II)2a**) to the only previously known structure **Ni(II)2c**.

The crystal packing motifs described here expand the list of known porphyrin aggregate structures, for example those based on π-stacking.[19] The clear dependence on central metal and substituents in the crystal structures is an indication for the variety of possible molecular arrangements which in less ordered materials. This may relate to the observation of differently sized and structured nanomaterials of porphyrins with different numbers of meso residues,[9b,c] the different types of structures observed for the interaction of porphyrins with π-conjugated surfaces[26] or electrooptical devices thereof.[27]

4. Experimental

4.1. General Information

General conditions and instrumentation were as described before.[10] All chemicals used were of analytical grade and purified before use. Dichloromethane was dried over phosphorous pentoxide followed by distillation; THF was dried over sodium followed by distillation. Silica gel 60 (Merck) was used for column chromatography. Analytical thin-layer chromatography (TLC) was carried out using silica gel 60 plates (fluorescence indicator F_{254}; Merck). Melting points are uncorrected and were measured with a Reichert Thermovar instrument. ^{1}H NMR spectra were recorded at frequencies of 250 (Bruker AM 270 instrument), 270 MHz (Bruker AM 270 instrument) or 500 MHz (Bruker AMX 500). Chemical shifts are given in ppm and referenced to the TMS signal as internal standard. The assignment of the signals was confirmed by 2D spectra (COSY, HMBC, HMQC) except for those porphyrins with low solubility. Electronic absorption spectra were recorded with a Specord S10 instrument (Zeiss) using CH_2Cl_2 as solvent. Mass spectra were recorded using a Varian MAT 711 or MAT 112 S mass spectrometer using the EI technique with direct insertion probe and excitation energy of 80 eV. FAB spectra were recorded with CH-5 DF instrument from Varian.

4.2. Starting Materials

The free base porphyrins **2c-g**, **3b** and **3d-e** were prepared as described previously by Ryppa *et al.*[4] The free base porphyrin **3f** was prepared as previously described by Song *et al.*[14] and the free base **2h** as described by Senge *et al.*[10]

4.3. Metallation Reactions

4.3.1. Nickel(II) and Copper(II) Insertion[13a]

The free base porphyrin (1 equiv.) was dissolved in DMF (50 mL) and heated to reflux with the appropriate metal(II) acetate (ca. 10 equiv.). The reaction was monitored by TLC control and the solvent removed under reduced pressure. The residue was dissolved in CH_2Cl_2 and the mixture filtered through silica gel, eluting with CH_2Cl_2. Finally, the solvent was removed under reduced pressure and the product dried in high vacuum.

4.3.2. Zinc(II) Insertion[13]

The free base porphyrin (1 equiv.) and zinc(II) oxide (2–3 equiv.) or zinc(II) acetate (1.5 equiv.) was dissolved in CH_2Cl_2 (50 mL) and treated with 3–5 drops of TFA. After stirring for 10 min the color of the reaction mixture changed from green to purple-red. The reaction was monitored by TLC control. The mixture was filtered through silica gel, eluting with CH_2Cl_2, followed by removal of the solvent reduced pressure. The product was dried in high vacuum.

4.4. Metalloporphyrins

*4.4.1. {5-(tert-Butyl)porphyrinato}nickel(II) (***Ni(II)2c***)*

The free base porphyrin **$H_2$2c** (50 mg, 0.14 mmol) was reacted with nickel(II) acetate and the crude product purified *via* column chromatography on silica gel (CH_2Cl_2 : *n*-hexane = 1 : 1, v/v) followed by recrystallization from CH_2Cl_2/MeOH. Yield: 57 mg (0.13 mmol, 98 %) of purple crystals. M.p.: >300 °C; R_f = 0.75 (CH_2Cl_2 : *n*-hexane = 2 : 1, v/v, silica gel, 6 × 3 cm); ^{1}H-NMR (270 MHz, $CDCl_3$): δ = 9.64 (AB, $^3J_{H\text{-}H}$ = 5.1 Hz, 2H, H_β), 9.59 (s, 1H, H_{meso}), 9.47 (s, 2H, H_{meso}), 9.10 (AB, $^3J_{H\text{-}H}$ = 4.4 Hz, 2H, H_β), 9.04 (AB, $^3J_{H\text{-}H}$ = 4.4 Hz, 2H, H_β), 8.97 (AB, $^3J_{H\text{-}H}$ = 5.1 Hz, 2H, H_β), 2.14 ppm (s, 9H, CH_3); ^{13}C-NMR (126 MHz, $CDCl_3$): δ = 141.64, 141.35, 141.17, 138.86, 133.04, 132.42, 131.83, 131.60, 122.91, 103.11, 102.98, 39.12, 38.76 ppm; UV/vis (CH_2Cl_2): λ_{max} (lg ε) = 404 (5.20), 530 (3.96), 567 nm (3.77); MS (EI, 220 °C, 80 eV): *m/z* = 422 (100 %, $[M]^{\bullet+}$), 407 (95 %, $[M - CH_3]^+$), 392 (18 %, $[M - C_2H_6]^{\bullet+}$), 366 (41 %, $[C_{24}H_{22}N_4]^{\bullet+}$), 183 (5 %, $[C_{24}H_{22}N_4]^{2+}$); HRMS (EI): *m/z* calcd. for $[C_{24}H_{20}N_4Ni]$: 422.1041; found 422.1075.

*4.4.2. {5(-tert-Butyl)porphyrinato}copper(II) (***Cu(II)2c***)*

The free base porphyrin **$H_2$2c** (58 mg, 0.16 mmol) was reacted with copper(II) acetate according to the standard procedure followed by recrystallization from CH_2Cl_2/MeOH. Yield: 49 mg (0.11 mmol, 72 %) of purple crystals. M.p.: 274 °C; R_f =

0.73 (CH_2Cl_2 : *n*-hexane = 2 : 1, v/v, silica gel, 6 × 3 cm); UV/vis (CH_2Cl_2): λ_{max} (lg ε) = 404 (5.44), 534 (4.00), 575 nm (3.65); MS (EI, 220 °C, 70 eV): *m/z* = 427 (89 %, $[M]^{\bullet+}$), 412 (100 %, $[M - CH_3]^+$), 397 (18 %, $[M - C_2H_6]^{\bullet+}$), 371 (69 %, $[C_{20}H_{12}N_4Cu]^{\bullet+}$), 214 (6 %, $[M]^{2+}$); HRMS (EI): *m/z* calcd. for $[C_{24}H_{20}N_4Cu]$ 427.0984; found 427.0977.

*4.4.3. {5-(tert-Butyl)porphyrinato}zinc(II) (***Zn(II)2c***)*

The free base porphyrin **$H_2$2c** (55 mg, 0.15 mmol) was reacted with zinc(II) oxide according to the standard procedure followed by recrystallization from CH_2Cl_2/MeOH. Yield: 31 mg (0.07 mmol, 47 %) of purple crystals. M.p.: 279 °C; R_f = 0.41 (CH_2Cl_2 : *n*-hexane = 2 : 1, v/v, silica gel, 6 × 3 cm); ^{1}H-NMR (270 MHz, $CDCl_3$): δ = 9.77 (AB, $^3J_{H\text{-}H}$ = 4.7 Hz, 2H, H_β), 9.58 (s, 1H, H_{meso}), 9.55 (s, 2H, H_{meso}), 9.01 (AB, $^3J_{H\text{-}H}$ = 4.4 Hz, 2H, H_β), 8.97 (AB, $^3J_{H\text{-}H}$ = 4.4 Hz, 2H, H_β), 8.87 (AB, $^3J_{H\text{-}H}$ = 4.7 Hz, 2H, H_β), 2.51 ppm (s, 9H, CH_3); ^{13}C-NMR (75 MHz, $CDCl_3$): δ = 149.62, 148.69, 148.33, 146.49, 131.46, 131.23, 130.86, 129.68, 127.93, 104.75, 104.09, 41.42, 41.05 ppm; UV/vis (CH_2Cl_2): λ_{max} (lg ε) = 405 (5.20), 495 (3.88), 540 (4.02), 583 nm (3.59); MS (EI, 70 eV): *m/z* = 428 (69 %, $[M]^{\bullet+}$), 413 (75 %, $[M - CH_3]^+$), 388 (100 %, $[M - C_3H_4]^+$), 372 (96 %, $[C_{20}H_{12}N_4Zn]^{\bullet+}$); HRMS (EI): *m/z* calcd. for $[C_{24}H_{20}N_4Zn]$ 428.0979; found 428.0983.

*4.4.4. (5-Hexylporphyrinato}nickel(II) (***Ni(II)2d***)*

The free base porphyrin **$H_2$2d** (42 mg, 0.11 mmol) was reacted with nickel(II) acetate and the crude product purified *via* column chromatography on silica gel (CH_2Cl_2 : *n*-hexane = 1 : 1, v/v) followed by recrystallization from CH_2Cl_2/MeOH. Yield: 42 mg (0.09 mmol, 87 %) of purple crystals. M.p.: >300 °C; R_f = 0.68 (CH_2Cl_2 : *n*-hexane = 1 : 1, v/v, silica gel, 6 × 3 cm); ^{1}H-NMR (300 MHz, $CDCl_3$): δ = 9.82 (s, 2H, H_{meso}), 9.81 (s, 1H, H_{meso}), 9.49 (AB, $^3J_{H\text{-}H}$ = 4.7 Hz, 2H, H_β), 9.20-9.19 (m, 6H, H_β), 4.72 (t, 2H, $^3J_{H\text{-}H}$ = 8.1 Hz, CH_2), 2.44-2.38 (m, 2H, CH_2), 1.73-168 (m, 2H, CH_2), 1.44-135 (m, 4H, CH_2), 0.92 ppm (t, 3H, $^3J_{H\text{-}H}$ = 7.2 Hz, CH_3); ^{13}C-NMR (75 MHz, $CDCl_3$): δ = 143.00, 142.16, 142.10, 142.06, 132.25, 132.15, 129.37, 118.57, 104.14, 103.21, 37.92, 34.63, 31.84, 30.23, 22.71, 14.12 ppm; UV/vis (CH_2Cl_2): λ_{max} (lg ε) = 394 (5.05), 511 (4.18), 543 nm (4.03); MS (EI, 220 °C, 70 eV): *m/z* = 450 (89 %, $[M]^{\bullet+}$), 379 (100 %, $[M - C_5H_{11}]^+$), 225 (2 %, $[M]^{2+}$), 190 (4 %, $[M - C_5H_{11}]^{2+}$); HRMS (EI): *m/z* calcd. for $[C_{26}H_{24}N_4Ni]$ 450.1354; found 450.1340.

*4.4.5. (5-Hexylporphyrinato}copper(II) (***Cu(II)2d***)*

The free base porphyrin **$H_2$2d** (42 mg, 0.11 mmol) was reacted with copper(II) acetate according to the standard procedure followed by recrystallization from CH_2Cl_2/MeOH. Yield: 40 mg (0.09 mmol, 82 %) of purple crystals. M.p.: 269 °C; R_f = 0.70 (CH_2Cl_2 : *n*-hexane = 1 : 1, v/v, silica gel, 6 × 3 cm); UV/vis (CH_2Cl_2): λ_{max} (lg ε) = 398 (6.22), 522 (4.10), 557 nm (3.62); MS (EI, 220 °C, 70 eV): *m/z* = 455 (51 %, $[M]^{\bullet+}$), 384 (100 %, $[M - C_5H_{11}]^+$), 192 (12 %, $[M - C_5H_{11}]^{2+}$); HRMS (EI): *m/z* calcd. for $[C_{26}H_{24}N_4Cu]$ 455.1297; found 455.1303.

*4.4.6. (5-Hexylporphyrinato}zinc(II) (***Zn(II)2d***)*

The free base porphyrin **$H_2$2d** (39 mg, 0.10 mmol) was reacted with zinc(II) oxide according to the standard procedure followed by column chromatography an silica (CH_2Cl_2 : *n*-hexane = 2 : 1, v/v) and recrystallization from CH_2Cl_2/hexane. Yield: 25 mg (0.05 mmol, 55 %) of purple crystals. M.p.: 259 °C (dec.); R_f = 0.47 (CH_2Cl_2 : *n*-hexane = 1 : 1, v/v, silica gel, 6 × 3 cm); ^{1}H-NMR (300 MHz, $CDCl_3$): δ = 10.02 (*s*, 2H, H_{meso}), 9.99 (*s*, 1H, H_{meso}), 9.58 (AB, $^3J_{H\text{-}H}$ = 4.7 Hz, 2H, H_β), 9.38-9.30 (*m*, 6H, H_β), 4.97 (t, $^3J_{H\text{-}H}$ = 8.1 Hz, 2H, CH_2), 2.56-2.53 (m, 2H, CH_2), 1.86-1.82 (m, 2H, CH_2), 1.49-1.44 (m, 4H, CH_2), 0.95 ppm (t, $^3J_{H\text{-}H}$ = 7.3 Hz, 3H, CH_3); ^{13}C-NMR (75 MHz, $CDCl_3$): δ = 149.42, 148.61, 131.95, 131.77, 131.66, 129.20, 120.81, 104.93, 38.44, 35.64, 31.96, 30.42, 22.79, 14.17 ppm; UV/vis (CH_2Cl_2): λ_{max} (lg ε) = 405 (5.10), 538 nm (4.16); MS (EI, 70 eV): *m/z*: = 456 (45 %, $[M]^{\bullet+}$), 385 (100 %, $[M - C_5H_{11}]^+$), 192 (5 %, $[M - C_5H_{11}]^{2+}$); HRMS (EI): *m/z* calcd. for $[C_{26}H_{24}N_4Zn]$ 456.1292; found 456.1279.

*4.4.7. {5-(1-Ethylpropyl)porphyrinato}nickel(II) (***Ni(II)2e***)*

The free base porphyrin **$H_2$2e** (16 mg, 0.04 mmol) was reacted with nickel(II) acetate and the crude product purified *via* column chromatography on silica gel (CH_2Cl_2 : *n*-hexane = 2 : 1, v/v) followed by recrystallization from CH_2Cl_2/MeOH. Yield: 16 mg (0.04 mmol, 93 %) of purple crystals. M.p.: 279-280 °C; R_f = 0.69 (CH_2Cl_2 : *n*-hexane = 2 : 1, v/v, silica gel, 6 × 3 cm); ^{1}H-NMR (500 MHz, $CDCl_3$): δ = 9.79 (s, 2H, H_{meso}), 9.78 (s, 1H, H_{meso}), 9.64 (AB, $^3J_{H\text{-}H}$ = 4.8 Hz, 2H, H_β), 9.21 (AB, $^3J_{H\text{-}H}$ = 4.8 Hz, 2H, H_β), 9.19 (br s, 4H, H_β), 4.72-4.67 (m, 1H, ethylpropyl-*CH*), 2.81-2.70 (m, 4H, CH_2), 0.89 ppm (t, $^3J_{H\text{-}H}$ = 7.4 Hz, 6H, CH_3); ^{13}C-NMR (126 MHz, $CDCl_3$): δ = 142.72, 141.78, 132.36, 132.22, 132.06, 130.58, 130.40, 121.25, 103.82, 102.95, 49.71, 33.89, 14.01 ppm; UV/vis (CH_2Cl_2): λ_{max} (lg ε) = 396 (5.36), 512 (4.14), 544 nm (3.73); MS (EI, 290 °C, 80 eV): *m/z* = 436 (78 %, $[M]^{\bullet+}$), 407 (100 %, $[M - C_2H_5]^+$), 392 (38 %, $[M - C_3H_8]^{\bullet+}$), 366 (31 %, $[M - C_5H_{10}]^+$), 218 (9 %, $[M]^{2+}$), 203 (6 %, $[M - C_2H_5]^{2+}$); HRMS (EI): *m/z* calcd. for $[C_{25}H_{22}N_4Ni]$ 436.1198; found 436.1176.

*4.4.8. {5-(1-Ethylpropyl)porphyrinato}copper(II) (***Cu(II)2e***)*

The free base porphyrin **$H_2$2e** (50 mg, 0.13 mmol) was reacted with copper(II) acetate according to the standard procedure followed by chromatography on silica gel (CH_2Cl_2 : *n*-hexane = 1 : 1, v/v) and recrystallization from CH_2Cl_2/hexane: 51 mg (0.11 mmol, 88 %) of purple crystals. M.p.: 312 °C; R_f = 0.85 (CH_2Cl_2 : *n*-hexane = 2 : 1, v/v, silica gel, 6 × 3 cm); UV/vis (CH_2Cl_2): λ_{max} (lg ε) = 397 (5.68), 522 (4.10), 557 nm (3.65); MS (EI, 220 °C, 70 eV): *m/z* = 441 (100 %, $[M]^{\bullet+}$), 412 (94 %, $[M - C_2H_5]^+$), 397 (26 %, $[M - C_3H_8]^{\bullet+}$), 371 (21 %, $[M - C_5H_{10}]^+$), 221 (7 %, $[M]^{2+}$), 206 (16 %, $[M - C_2H_5]^{2+}$); HRMS (EI): *m/z* calcd. for $[C_{25}H_{22}N_4Cu]$ 441.1140; found 441.1149.

*4.4.9. {5-(1-Ethylpropyl)porphyrinato}zinc(II) (***Zn(II)2e***)*

The free base porphyrin **$H_2$2e** (59 mg, 0.15 mmol) was reacted with zinc(II) oxide according to the standard procedure followed by column chromatography an silica (CH_2Cl_2 : *n*-hexane = 1 : 1, v/v) and recrystallization from CH_2Cl_2/hexane. Yield: 46 mg (0.10 mmol, 68 %) of purple crystals. M.p.: 325 °C (dec.); R_f = 0.64 (CH_2Cl_2 : *n*-hexane

= 2 : 1, v/v, silica gel, 6 × 3 cm); ^{1}H-NMR (500 MHz,$CDCl_3$): δ = 10.18 (s, 2H, H_{meso}), 10.02 (s, 1H, H_{meso}), 9.95 (AB, $^{3}J_{H\text{-}H}$ = 4.4 Hz, 2H, H_{β}), 9.49 (AB, $^{3}J_{H\text{-}H}$ = 4.4 Hz, 2H, H_{β}), 9.37-9.34 (m, 4H, H_{β}), 5.31-5.25 (m, 1H, ethylpropyl-*CH*), 2.81-2.70 (m, 4H, CH_2), 0.89 ppm (t, $^{3}J_{H\text{-}H}$ = 7.4 Hz, 6H, CH_3); ^{13}C-NMR (126 MHz, $CDCl_3$): δ = 149, 131, 124.42, 105.19, 104.89, 103.89, 50.72, 35.07, 14.38 ppm; UV/vis (CH_2Cl_2): λ_{max} (lg ε) = 401 (5.43), 532 (4.16), 563 nm (3.37); MS (EI, 70 eV): *m/z* = 442 (60 %, $[M]^{\bullet+}$), 413 (100 %, $[M - C_2H_5]^{+}$), 398 (46 %, $[M - C_3H_8]^{\bullet+}$), 372 (28 %, $[M - C_5H_{10} + H]^{\bullet+}$), 207 (5 %, $[M - C_2H_5]^{2+}$), 199 (9 %, $[M - C_3H_8]^{2+}$), 186 (2 %, $[M - C_5H_{10} + H]^{2+}$); HRMS (EI): *m/z* calcd. for $[C_{25}H_{22}N_4Zn]$ 442.1136; found 442.1118.

4.4.10. (5-Phenylporphyrinato}nickel(II) (**Ni(II)2f**)

The free base porphyrin **$H_2$2f** (50 mg, 0.11 mmol) was reacted with nickel(II) acetate following the general procedure. Purification involved recrystallization from CH_2Cl_2/MeOH. Yield: 21 mg (0.05 mmol, 37 %) of purple crystals. M.p.: >310 °C; R_f 0.65 (CH_2Cl_2 : *n*-hexane = 2 : 1, v/v, silica gel, 6 × 3 cm); ^{1}H-NMR (300 MHz, $CDCl_3$): δ= 10.00 (s, 2H, H_{meso}), 9.99 (s, 1H, H_{meso}), 9.30 (br s, 4H, H_{β}), 9.21 (AB, $^{3}J_{H\text{-}H}$ = 4.7 Hz, 2H, H_{β}), 8.95 (AB, $^{3}J_{H\text{-}H}$ = 4.7 Hz, 2H, H_{β}), 8.10-8.04 (m, 2H, Ph-*H*), 7.76-7.68 ppm (m, 3H, Ph-*H*). ^{13}C-NMR (75 MHz, $CDCl_3$): δ = 142.64, 133.89, 132.41, 132.37, 131.94, 127.75, 126.81, 104.75, 103.94 ppm; UV/vis (CH_2Cl_2): λ_{max} (lg ε) = 392 (5.29), 509 (4.17), 541 nm (4.09); MS (EI, 220 °C, 80 eV): *m/z* = 442 (100 %, $[M]^{\bullet+}$), 221 (8 %, $[M]^{2+}$); HRMS (EI): *m/z* calcd. for $[C_{26}H_{16}N_4Ni]$ 442.0728; found 442.0725.

4.4.11. (5-Phenylporphyrinato}copper(II) (**Cu(II)2f**)

The free base porphyrin **$H_2$2f** (50 mg, 0.11 mmol) was reacted with copper(II) acetate following the general procedure. Purification involved recrystallization from CH_2Cl_2/MeOH. Yield: 37 mg (0.08 mmol, 64 %) of purple crystals. M.p.: >310 °C; R_f = 0.68 (CH_2Cl_2 : *n*-hexane = 2 : 1, v/v, silica gel, 6 × 3 cm); UV/vis (CH_2Cl_2): λ_{max} (lg ε) = 397 (5.50), 521 (4.11), 555 nm (3.79); MS (EI, 220 °C, 80 eV): *m/z* = 447 (100 %, $[M]^{\bullet+}$), 224 (8 %, $[M]^{2+}$); HRMS (EI): *m/z* calcd. for $[C_{26}H_{16}N_4Cu]$ 447.0671; found 447.0637).

4.4.12. (5-Phenylporphyrinato}zinc(II) (**Zn(II)2f**)

The free base porphyrin **$H_2$2f** (48 mg, 0.12 mmol) was reacted with zinc oxide acetate following the general procedure. Purification involved recrystallization from CH_2Cl_2/MeOH. Yield: 22 mg (0.05 mmol, 39 %) of purple crystals. M.p.: >310 °C; R_f = 0.51 (CH_2Cl_2 : *n*-hexane = 2 : 1, v/v, silica gel, 6 × 3 cm); ^{1}H-NMR (300 MHz, $CDCl_3$): δ = 10.35-10.31 (m, 3H, H_{meso}), 9.55-9.16 (m, 8H, H_{β}), 8.26-8.23 (m, 2H, Ph-*H*), 7.80-7.77 ppm (m, 3H, Ph-*H*); UV/vis (CH_2Cl_2): λ_{max} (lg ε) = 402 (5.42), 531 (4.05), 563 nm (3.35); MS (EI, 220 °C, 80 eV) *m/z*: 448 (100 %, $[M]^{\bullet+}$), 224 (35 %, $[M]^{2+}$); HRMS (EI): *m/z* calcd. for $[C_{26}H_{16}N_4Zn]$ 448.0666; found 448.0660.

4.4.13. {5-(4-Methoxyphenyl)porphyrinato}nickel(II) (**Ni(II)2g**)

The free base porphyrin **$H_2$2g** (105 mg, 0.25 mmol) was reacted with nickel(II) acetate following the general procedure. Purification involved recrystallization from CH_2Cl_2/MeOH. Yield: 98 mg (0.21 mmol, 82 %) of purple crystals. M.p.: 321 °C; R_f = 0.61 (CH_2Cl_2 : *n*-hexane = 2 : 1, v/v, silica gel, 6 × 3 cm); ^{1}H-NMR (500 MHz, $CDCl_3$): δ= 9.98 (s, 2H, H_{meso}), 9.96 (s, 1H, H_{meso}), 9.32-9.27 (m, 4H, H_β), 9.20 (AB, $^3J_{H\text{-}H}$ = 4.8 Hz, 2H, H_β), 8.98 (*AB*, $^3J_{H\text{-}H}$ = 4.8 Hz, 2H, H_β), 8.00-7.95 (m, 2H, Ph-*H*), 7.28-7.22 (m, 2H, Ph-*H*), 4.07 ppm (s, 3H, CH_3); ^{13}C-NMR (126 MHz, $CDCl_3$): δ= 159.43, 143.01, 142.69, 142.55, 134.88, 133.54, 132.39, 132.37, 132.36, 118.58, 112.35, 104.69, 103.83, 55.58 ppm; UV/vis (CH_2Cl_2): λ_{max} (lg ε) = 394 (5.35), 510 (4.15), 542 nm (4.00); MS (EI, 290 °C, 80 eV): *m/z* = 472 (100 %, $[M]^{\bullet+}$), 457 (10 %, $[M - CH_3]^+$), 441 (2 %, $[M - OCH_3]^+$), 236 (10 %, $[M]^{2+}$), 228 (2 %, $[M - CH_3]^{2+}$); HRMS (EI): *m/z* calcd. for [$C_{27}H_{18}N_4ONi$] 472.0834; found 472.0857.

4.4.14. {5-(4-Methoxyphenyl)porphyrinato}copper(II) (**Cu(II)2g**)

The free base porphyrin **$H_2$2g** (47 mg, 0.11 mmol) was reacted with copper(II) acetate following the general procedure. Purification involved silica gel column chromatography on silica gel (eluent: CH_2Cl_2 : *n*-hexane = 1 : 1, v/v) and recrystallization from CH_2Cl_2/MeOH. Yield: 44 mg (0.09 mmol, 82 %) of purple crystals. M.p.: >330 °C; R_f = 0.91 (CH_2Cl_2 : *n*-hexane = 2 : 1, v/v, silica gel, 6 × 3 cm); UV/vis (CH_2Cl_2): λ_{max} (lg ε) = 398 (5.35), 522 (4.11), 555 nm (3.66); MS (EI, 210 °C, 70 eV) *m/z*: 477 (100 %, $[M]^{\bullet+}$), 239 (14 %, $[M]^{2+}$); HRMS (EI): *m/z* calcd. for [$C_{27}H_{19}N_4OCu$] 478.0855; found 478.0885.

4.4.15. {5-(4-Methoxyphenyl)porphyrinato}zinc(II) (**Zn(II)2g**)

The free base porphyrin **$H_2$2g** (105 mg, 0.25 mmol) was reacted with zinc oxide following the general procedure. Purification involved column chromatography on silica gel (eluent: ethyl acetate : *n*-hexane = 1 : 4, v/v) and recrystallization from CH_2Cl_2/MeOH. Yield: 48 mg (0.10 mmol, 95 %) of purple crystals. M.p.: >330 °C; R_f = 0.36 (CH_2Cl_2 : *n*-hexane = 2 : 1, v/v, silica gel, 6 × 3 cm); ^{1}H-NMR (300 MHz, $CDCl_3$): δ= 10.29 (s, 2H, H_{meso}), 10.22 (s, 1H, H_{meso}), 9.52-9.47 (m, 4H, H_β), 9.44 (AB, $^3J_{H\text{-}H}$ = 4.5 Hz, 2H, H_β), 9.19 (AB, $^3J_{H\text{-}H}$ = 4.5 Hz, 2H, H_β), 8.17 (AB, $^3J_{H\text{-}H}$ = 8.7 Hz, 2H, Ph-*H*), 7.33 (AB, $^3J_{H\text{-}H}$ = 8.7 Hz, 2H, Ph-*H*), 4.12 ppm (s, 3H, OCH_3); ^{13}C-NMR (75 MHz, $CDCl_3$): δ = 155.90, 135.61, 132, 112.19, 105.60, 105.47, 55.65 ppm; UV/vis (CH_2Cl_2): λ_{max} (lg ε) = 404 (5.50), 532 (4.14), 563 nm (3.41); MS (EI, 220 °C, 70 eV): *m/z* = 478 (100 %, $[M]^{\bullet+}$), 463 (9 %, $[M - CH_3]^+$); HRMS (EI): *m/z* calcd. for [$C_{27}H_{18}N_4OZn$)] 478.0772; found 478.0761.

4.4.16. (5-(3,5-Di-tert-butyl)porphyrinato)nickel(II) (**Ni(II)2h**)

The free base porphyrin **$H_2$2h** (300 mg, 0.602 mmol) was dissolved in toluene (30 mL) 100 mL RBF. The solution was heated to 120 °C before $Ni(acac)_2$ (464 mg, 1.806 mmol) was added. The reaction was stirred at this temperature 4 h, monitoring via TLC control. The reaction was then cooled to room temperature and solvents were removed in vacuo. The crude residue was redissolved in CH_2Cl_2 and filtered through a short plug of

silica gel using CH_2Cl_2 as eluent. The solvent was removed *in vacuo* and the residue was recrystallized from CH_2Cl_2/MeOH. Yield: 282 mg (0.507 mmol, 84 %) of purple-red crystals. R_f (CH_2Cl_2 : hexane = 1:1, v/v): 0.76; ^{1}H NMR (400 MHz, $CDCl_3$ + pyridine-D_5 = 20:1, v/v): δ = 9.98 ppm (s, 2H, H_{meso}), 9.95 (s, 1H, H_{meso}), 9.28 (br. s, 4H, H_β), 9.20 (d, J = 4.7 Hz, 2H, H_β), 9.00 (d, J = 4.7 Hz, 2H, H_β), 7.94 (d, J = 1.8 Hz, 2H, aryl-*H*), 7.77 (t, J = 1.8 Hz, 1H, aryl-*H*), 1.51 (s, 18H, *t*-butyl-*H*); ^{13}C NMR (100 MHz, $CDCl_3$): δ = 31.7, 35.0, 103.7, 104.6, 120.2, 121.1, 129.0, 131.8, 132.2, 132.3, 132.7, 140.1, 142.5, 142.6, 142.8, 142.9, 148.9 ppm; UV/vis (CH_2Cl_2): λ_{max} (log ε) = 394 (5.25), 510 (4.10), 544 nm (3.98); HRMS (MALDI): *m/z* = 554.1980 calcd. for $C_{34}H_{32}N_4Ni$; found 554.2001.

4.4.17. {5,15-Di(iso-butyl)porphyrinato}copper(II) (**Cu(II)3b**)

The free base porphyrin **$H_2$3b** (60 mg, 0.14 mmol) was dissolved in dichloromethane (60 mL) and mixed with methanol (30 mL), water (3 drops) and copper acetate (79.2 mg, 0.44 mmol). The mixture was stirred at rt for 12 h followed by filtration through silica gel (CH_2Cl_2). Column chromatography on silica gel (CH_2Cl_2 : *n*-hexane = 1:2, v/v) gave a single product fraction, which yielded red crystals after recrystallization from CH_2Cl_2/MeOH. Yield: 36 mg (0.07 mmol, 52 %). M.p.: >300 ºC; R_f = 0.38 (CH_2Cl_2 : *n*-hexane = 1 : 2, v/v, silica gel); UV/vis (CH_2Cl_2): λ_{max} (lg ε) = 404 (5.66), 529 (4.08), 564 nm (3.11); MS (EI, 70 eV): *m/z* = 438 (8 %, $[M]^+$), 440 (24 %, $[M - C_3H_7]^+$), 397 (20 %, $M - C_6H_{14}]^+$), 243 (3 %, $[M]^{2+}$); HRMS (EI): *m/z* calcd. for $[C_{28}H_{28}CuN_4]$ 483.1609; found 483.1592).

4.4.18. (5,15-Dihexylporphyrinato)nickel(II) (**Ni(II)3d**)

The free base porphyrin **$H_2$3d** (35 mg, 0.07 mmol) was reacted with nickel(II) acetate and the crude product purified via column chromatography on silica gel (ethyl acetate : *n*-hexane = 1 : 4, v/v) followed by recrystallization from CH_2Cl_2/MeOH. Yield: 23 mg (0.04 mmol, 59 %) of purple crystals. M.p.: 215 °C; R_f = 0.93 (CH_2Cl_2 : *n*-hexane = 2 : 1, v/v, silica gel, 6 × 3 cm); ^{1}H-NMR (400 MHz, $CDCl_3$): δ = 9.74 (s, 2H, H_{meso}), 9.47 (AB, $^3J_{H\text{-}H}$ = 4.7 Hz, 4H, H_β), 9.20 (AB, $^3J_{H\text{-}H}$ = 4.7 Hz, 4H, H_β), 4.69 (t, $^3J_{H\text{-}H}$ = 8.1 Hz, 4H, CH_2), 2.41-2.35 (m, 4H, CH_2), 1.72-1.65 (m, 4H, CH_2), 1.51-1.34 (m, 8H, CH_2), 0.92 ppm (t, $^3J_{H\text{-}H}$ = 7.2 Hz, 6H, CH_3); ^{13}C-NMR (75 MHz, $CDCl_3$): δ = 142.53, 141.38, 132.06, 129.31, 117.26, 103.83, 37.06, 34.21, 31.81, 30.14, 22.70, 14.12 ppm; UV/vis (CH_2Cl_2): λ_{max} (lg ε) = 402 (5.37), 518 (4.12), 549 nm (3.63); MS (EI, 220 °C, 70 eV): *m/z* = 534 (100 %, $[M]^{\bullet+}$), 463 (92 %, $[M - C_5H_{11}]^+$), 392 (87 %, $[M - 2\ C_5H_{11}]^{\bullet+}$), 267 (2 %, $[M]^{2+}$); HRMS (EI): *m/z* calcd. for $[C_{32}H_{36}N_4Ni]$ 534.2293; found 534.2271.

4.4.19. (5,15-Dihexylporphyrinato)copper(II) (**Cu(II)3d**)

The free base porphyrin **$H_2$3d** (44 mg, 0.09 mmol) was reacted with copper(II) acetate and the crude product purified *via* column chromatography on silica gel (ethyl acetate : *n*-hexane = 1 : 4, v/v) followed by recrystallization from CH_2Cl_2/MeOH. Yield: 47 mg (0.09 mmol, 95 %) of purple crystals. M.p.: 161 °C; R_f = 0.96 (CH_2Cl_2 : *n*-hexane = 2 : 1, v/v, silica gel, 6 × 3 cm); UV/vis (CH_2Cl_2): λ_{max} (lg ε) = 404 (5.56), 530 nm (4.13); MS (EI, 220 °C, 70 eV): *m/z* = 539 (100 %, $[M]^{\bullet+}$), 468 (86 %, $[M - C_5H_{11}]^+$), 397

(50 %, $[M - 2\ C_5H_{11}]^{\bullet+}$), 270 (5 %, $[M]^{2+}$), 234 (9 %, $[M - C_5H_{11}]^{2+}$), 199 (13 %, $[M - 2\ C_5H_{11}]^{2+}$); HRMS (EI): *m/z* calcd. for $[C_{32}H_{36}N_4Cu]$ 539.2236; found 539.2209.

*4.4.20. (5,15-Dihexylporphyrinato)zinc(II) (***Zn(II)3d***)*

The free base porphyrin **$H_2$3d** (250 mg, 0.52 mmol) was reacted with zinc(II) acetate. The mixture was washed with several portions of water and the organic layer was dried over sodium sulfate and filtered. The solvent was removed under reduced pressure until crystals were formed which were recrystallization from CH_2Cl_2/MeOH. Yield: 250 mg (0.462 mmol, 89 %) of purple crystals. M.p.: 285 °C (dec.); R_f = 0.83 (CH_2Cl_2 : *n*-hexane = 2 : 1, v/v, silica gel, 6 × 3 cm); ^{1}H-NMR (400 MHz, $CDCl_3$): δ = 10.23 (br s, 2H, H_{meso}), 9.60-9.59 (m, 4H, H_β), 9.43-9.42 (m, 4H, H_β), 5.05-5.01 (m, 4H, CH_2), 2.57-2.55 (m, 4H, CH_2), 1.86-1.83 (m, 4H, CH_2), 1.58-1.39 (m, 8H, CH_2), 0.97-0.94 ppm (m, 6H, CH_3); UV/vis (CH_2Cl_2): λ_{max} (lg ε) = 408 (5.58), 540 (4.17), 615 nm (3.76); MS (EI, 220 °C, 70 eV) *m/z*: 540 (50 %, $[M]^{\bullet+}$) , 469 (100 %, $[M - C_5H_{11}]^+$), 398 (84 %, $[M - 2\ C_5H_{11}]^{\bullet+}$), 200 (9 %, $[M - 2\ C_5H_{11}]^{2+}$); HRMS (EI): *m/z* calcd. for $[C_{32}H_{36}N_4Zn]$ 540.2231; found 540.2205.

*4.4.21. {5,15-Bis(1-ethylpropyl)porphyrinato}copper(II) (***Cu(II)3e***)*

The free base porphyrin **$H_2$3e** (50 mg, 0.12 mmol) was dissolved in dichloromethane (60 mL) and mixed with methanol (25 mL), water (3 drops) and copper acetate (67.5 mg, 0.37 mmol). The mixture was stirred at rt for 2 h followed by filtration through silica gel (CH_2Cl_2). Recrystallization from CH_2Cl_2/MeOH gave red crystals. Yield: 35 mg (0.07 mmol, 63 %). M.p.: >310 ºC; R_f = 0.69 (CH_2Cl_2 : *n*-hexane = 1 : 2, v/v, silica gel); UV/vis (CH_2Cl_2): λ_{max} (lg ε) = 404 (5.85), 530 (4.24), 567 nm (3.31); MS (EI, 70 eV): *m/z* = 516 (6 %, $[M]^+$), 482 (8 %, $[M - C_2H_5]^+$), 411 (13 %, $M - C_7H_{16}]^+$), 396 (9 %, $M - C_8H_{19}]^+$), 256 (13 %, $[M]^{2+}$); HRMS (EI): *m/z* calcd. for $[C_{30}H_{32}CuN_4]$ 511.1923; found 511.1907.

*4.4.22. (5,15-Diphenylporphyrinato)nickel(II) (***Ni(II)3f***)*[14]

The free base porphyrin **$H_2$3f** (250 mg: 0.54 mmol) was reacted with nickel(II) acetate following the general procedure. Purification involved recrystallization from CH_2Cl_2/MeOH. Yield: 220 mg (0.426 mmol, 79 %) of purple crystals. R_f = 0.72 (CH_2Cl_2 : *n*-hexane = 2 : 1, v/v, silica gel, 6 × 3 cm); (400 MHz: $CDCl_3$) δ = 9.96 (s, 2H, H_{meso}), 9.21 (s, 4H, H_β), 8.96 (s, 4H, H_β), 8.07 (d, 4H, Ph-*H*), 7.77-7.73 ppm (m, 6H, Ph-*H*); UV/vis (CH_2Cl_2): λ_{max} (lg ε) = 400 (4.73), 515 (4.08), 547 nm (3.79); MS (EI, 210 °C, 70 eV): *m/z* = 518 (100 %, $[M]^{\bullet+}$), 440 (20 %, $[M - C_6H_6]^{\bullet+}$), 259 (3 %, $[M]^{2+}$). Other analytical data were as reported in the literature.[14]

*4.3.23. (5,15-Diphenylporphyrinato)copper(II) (***Cu(II)3f***)*[20]

The free base porphyrin **$H_2$3f** (250 mg, 0.54 mmol) was reacted with copper(II) acetate following the general procedure. Purification involved recrystallization from CH_2Cl_2/MeOH. Yield: 210 mg (0.4 mmol, 75 %) of purple crystals. R_f = 0.68 (CH_2Cl_2 : *n*-hexane = 2 : 1, v/v, silica gel, 6 × 3 cm); UV/vis (CH_2Cl_2): λ_{max} (lg ε) = 403 (3.99), 526

(3.69), 591 nm (3.41); MS (EI, 210 °C, 70 eV): *m/z* = 523 (100 %, $[M]^{\bullet+}$), 445 (22 %, $[M - C_6H_6]^{\bullet+}$), 260 (48 %, $[M]^{2+}$), 223 (16 %, $[M - C_6H_6]^{2+}$). Other analytical data were as reported in the literature.[20]

*4.3.24. (5,15-Diphenylporphyrinato)zinc(II) (***Zn(II)3f***)*[20]

The free base porphyrin **$H_2$3f** (200 mg, 0.44 mmol) was reacted with zinc acetate following the general procedure. Purification involved recrystallization from CH_2Cl_2/MeOH. Yield: 210 mg (0.41 mmol, 93 %) of purple crystals. R_f = 0.39 (CH_2Cl_2 : *n*-hexane = 2 : 1, v/v, silica gel, 6 × 3 cm); (400 MHz: $CDCl_3$) δ = 10.34 (s, 2H, H_{meso}), 9.47 (d, $^3J_{H\text{-}H}$ = 4.64 Hz, 4H, H_β), 9.18 (d, $^3J_{H\text{-}H}$ = 4.64Hz, 4H, H_β), 8.30 (dd, $^3J_{H\text{-}H}$ = 1.16, 2.32 Hz, 4H, Ph-*H*), 7.85-7.82 ppm (m, 6H, Ph-*H*); UV/vis (CH_2Cl_2): λ_{max} (lg ε) = 407 (4.84), 536 (3.66), 571 nm (2.97); MS (EI, 210 °C, 70 eV): *m/z* = 524 (100 %, $[M]^{\bullet+}$), 446 (19 %, $[M - C_6H_6]^{\bullet+}$), 262 (21 %, $[M]^{2+}$). Other analytical data were as reported in the literature.[20]

4.5. Single crystal X-Ray structure determinations

Growth and handling of crystals followed the concept developed by Hope.[24] The intensities were corrected for Lorentz, polarization and absorption effects. Nonhydrogen atoms were refined with anisotropic thermal parameters, and hydrogen atoms were placed into geometrically calculated positions and refined using a riding model. The structures were solved with Direct Methods or Patterson synthesis using the SHELXL PLUS program system and refined against $|F^2|$ with the program SHELX using all data.[25] Hydrogen atoms were fixed geometrically and allowed to ride on the parent carbon atoms, with aromatic C-H = 0.93 Å, methylene C-H = 0.97 Å and methyl C-H = 0.97 Å. The displacement parameters were set for aromatic H atoms at $U_{iso}(H) = 1.2\ U_{eq}(C)$, methylene H atoms at $U_{iso}(H) = 1.2U_{eq}(C)$ and methyl H atoms at $U_{iso}(H) = 1.5\ U_{eq}(C)$.

*4.5.1. Crystal data and refinement (***Ni(II)2a***)*

Crystal data: $C_{24}H_{20}N_4Ni$, M = 423.15, monoclinic, space group *C2/c*, a = 50.9305(18), b = 6.5230(2), c = 11.5664(3) Å, α = 90°, β = 95.7323(19)°, γ = 90°, V = 3823.4(2) Å^3, Z = 8, T = 90K, μ(MoK_α) = 0.1033 cm^{-1}, 21627 reflections measured, 5573 unique reflections measured (R_{int} = 0.1175), 276 parameters, 3007 reflections with $I > 2.0\sigma(I)$, refinement against $|F^2|$, *R*1 ($I > 2.0\sigma(I)$) = 0.0891, *wR*2 (all data) = 0.2850, S = 1.095, ρ_{max} = 1.470. *Refinement:* Constraints and restraints were used to model the disorder in the *n*-butyl chain C21 - C24 (EADP, DFIX, ISOR, SADI) and the model was refined to convergence. High residuals were located near the Ni center.

*4.5.2. Crystal data and refinement (***Zn(II)2e***)*

Crystal data: $C_{25}H_{22}N_4Zn$, M = 443.83, monoclinic, space group $P2_1/c$, a = 14.4616(15), b = 12.1750(13), c = 11.9296(13) Å, α = 90°, β = 112.684(2)°, γ = 90°, V = 1938.0(4) Å^3, Z = 4, T = 90K, μ(MoK_α) = 0.1288 cm^{-1}, 17123 reflections measured, 4456 unique reflections measured (R_{int} = 0.0558), 274 parameters, 3348 reflections with $I > 2.0\sigma(I)$, refinement against $|F^2|$, *R*1 ($I > 2.0\sigma(I)$) = 0.0376, *wR*2 (all data) = 0.0940, S =

1.018, ρ_{max} = 1.521 *Refinement:*. Residual electron density was located in the side chain region which shows higher librational movement for some atoms. The close contacts are due to the very tight dimeric packing of the molecules in the crystal.

*4.5.3. Crystal data and refinement (***Zn(II)2f***)*

Crystal data: $C_{79}H_{52}N_{12}Zn_3$, M = 1381.43, monoclinic, space group $P2_1/c$, a = 28.441(3), b = 18.5464(16), c = 11.4645(10) Å, α = 90°, β = 91.320(2)°, γ = 90°, V = 6045.7(9) Å^3, Z = 4, T = 90K, μ(MoK$_\alpha$) = 0.1243 cm^{-1}, 68676 reflections measured, 13846 unique reflections measured (R_{int} = 0.0769), 871 parameters, 9701 reflections with $I > 2.0\sigma(I)$, refinement against $|F^2|$, $R1$ ($I > 2.0\sigma(I)$) = 0.0666, $wR2$ (all data) = 0.1925, S = 1.096, ρ_{max} = 1.483. *Refinement:* Structure was refined as a two component twin. Restraints were used to model the disordered solvent methanol molecules C1s-C4s and O1s-O4s (DFIX) and the model was refined to convergence.

*4.5.4. Crystal data and refinement (***Ni(II)2h***)*

Crystal data: $C_{69}H_{65}Cl_3N_8Ni_2^-$, M = 1230.06, orthorhombic, space group $P2_12_12_1$, a = 11.0604(4), b = 25.9552(8), c = 41.0751(13) Å, α = 90°, β = 90°, γ = 90°, V = 11790.3(7) Å^3, Z = 8, T = 100K, μ(MoK$_\alpha$) = 0.0825 cm^{-1}, 131133 reflections measured, 23278 unique reflections measured (R_{int} = 0.0434), 1595 parameters, 20473 reflections with $I > 2.0\sigma(I)$, refinement against $|F^2|$, $R1$ ($I > 2.0\sigma(I)$) = 0.0374, $wR2$ (all data) = 0.0835, S = 1.037, ρ_{max} = 1.386. *Refinement:* Refined as a two component inversion twin. Restraints were used (ISOR) to model the disorder tert-butyl groups over two positions each with occupancies of 79, 68 and 65% for the major moieties and refined to convergence. Solvent molecules were found packed between porphyrin layers.

4.6. Normal structural decomposition (NSD) analysis

The overall degree of distortion and the contributions of individual distortion modes were determined using the normal structural decomposition method developed by Shelnutt and coworkers.[20] NSD classifies the distortions in terms of equivalent displacements along the normal coordinates and illustrates the mix of distortion modes present in porphyrins.

Acknowledgement

This work was supported by a grant from Science Foundation Ireland (SFI IvP 13/IA/1894 SFI). We are indebted to Dr. J. Fettinger and Prof. M. M. Olmstead (UC Davis) for help with some of the data collections.

Supplementary Material

CCDC 1414355 (**Ni(II)2a**), 1414356 (**Zn(II)2e**), 1414357 (**Zn(II)2f**) and 1414358 (**Ni(II)2h**) contain the supplementary crystallographic data for this paper. These data can be obtained free of charge from The Cambridge Crystallographic Data Centre *via* www.ccdc.cam.ac.uk/data_request/cif.

References and Notes

1 Scheidt, W. R.; Lee, Y. J. *Struct. Bonding (Berlin)* **1987**, *64*, 1-70.

2 (a) Senge, M. O. *Chem. Commun.* **2006**, 243-256; (b) Senge, M. O. In *The Porphyrin Handbook*; Kadish, K. M.; Smith, K. M.; Guilard, R., Eds.; Academic Press, San Diego, 2000, Vol. 1, pp 239-347; (c) Lebedev, A. Y.; Filatov, M. A.; Cheprakov, A. V.; Vinogradov, S. A., *J. Phys. Chem. A* **2008**, *112*, 7723-7733; (d) Senge, M. O.; MacGowan, S. A.; O'Brien, J. M. *Chem. Commun.* **2015**, in press, doi 10.1039/C5CC06254C.

3 (a) Senge, M. O.; Davis, M. *J. Porphyrins Phthalocyanines* **2010**, *14*, 557-567; (b) Ptaszek, M.; McDowell, B. E.; Taniguchi, M.; Kim, H.-j.; Lindsey, J. S., *Tetrahedron* **2007**, *63*, 3826-3839.

4 Ryppa, C.; Senge, M. O.; Hatscher, S. S.; Kleinpeter, E.-P.; Wacker, P.; Schilde, U.; Wiehe, A. *Chem. Eur. J.* **2005**, *11*, 3427-3442.

5 Senge, M. O. *Chem. Commun.* **2011**, *47*, 1943-1960.

6 (a) Wiehe, A.; Ryppa, C.; Senge, M. O. *Org. Lett.* **2002**, *4*, 3807-3809; (b) Hatscher, S.; Senge, M. O. *Tetrahedron Lett.* **2003**, *44*, 157-160.

7 (a) Lindsey, J. S. *Acc. Chem. Res.* **2010**, *43*, 300-311; (b) Senge, M. O. *Acc. Chem. Res.* **2005**, *38*, 733-743.

8 Brinas, R. P.; Brückner, C. *Tetrahedron* **2002**, *58*, 4375-4381.

9 (a) Fang, Y.; Senge, M. O., Van Caemelbecke, E.; Smith, K. M.; Medforth, C. J.; Zhang, M.; Kadish, K. M. *Inorg. Chem.* **2014**, *53*, 10772-10778; (b) Reddy, M. H. V.; Al-Shammari, R. M.; Al-Attar, N.; Kennedy, E.; Rogers, L.; Lopez, S.; Senge, M. O.; Keyes, T. E.; Rice, J. H. *Phys. Chem. Chem. Phys.* **2014**, *16*, 4386-4393; (c) Reddy, H. V.; Al-Shammari, R. M.; Al-Attar, N.; Rogers, L.; Lopez, S.; Forster, R. J.; Senge, M. O.; Keyes, T. E.; Rice, J. H. *Chem. Phys. Mater.* **2014**, *143*, 963-968.

10 Senge, M. O.; Shaker, Y. M.; Pintea, M.; Ryppa, C.; Hatscher, S. S.; Ryan, A.; Sergeeva, Y. *Eur. J. Org. Chem.* **2010**, 237-258.

11 Senge, M. O.; Dahms, K.; Holdt, H.-J.; Kelling, A. *Z. Naturforsch.* **2015**, *70b*, 119-123.

12 (a) Song, X.-Z.; Jentzen, W.; Jaquinod, L.; Khoury, R. G.; Medforth, C. J.; Jia, S.-L.; Ma, J.-G.; Smith, K. M.; Shelnutt, J. A. *Inorg. Chem.* **1998**, *37*, 2117-2128; (b) Senge, M. O. *Acta Cryst.* **2011**, *C67*, m39-m42.

13 (a) Buchler, J. W. In *The Porphyrins*; Dolphin, D., Ed.; Academic Press: New York, 1978, Vol. 1, pp 389-483; (b) Speck, M.; Niethammer, D.; Senge, M. O. *J. Chem. Soc., Perkin Trans. 2* **2002**, 455-462.

14 Song, X.-Z.; Jentzen, W.; Jia, S.-L.; Jaquinod, L.; Nurco, D. J.; Medforth, C. J.; Smith, K. M.; Shelnutt, J. A. *J. Am. Chem. Soc.* **1996**, *118*, 12975-12988.

15 (a) Rothemund, P. *J. Am. Chem. Soc.* **1935**, *57*, 2010-2011; (b) Volz, H.; Herb, G. *Z. Naturforsch.* **1983**, *38b*, 1240-1242; (c) Senge, M. O.; Bischoff, I.; Nelson, N. Y.; Smith, K. M. *J. Porphyrins Phthalocyanines* **1999**, *3*, 99-116.

16 Senge, M. O.; Forsyth, T. P.; Smith, K. M. *Z. Kristallogr.* **1996**, *211*, 176-185.

17 Kozlowski, P.M.; Bingham, J. R.; Jarzecki, A. A. *J. Phys. Chem. A*, **2008**, *112*, 12781–12788.

18 Fleischer, E. B.; Miller, C. K.; Webb, L. E. *J. Am. Chem. Soc.*, **1964**, *86*, 2342-2347.

19 Senge, M. O.; Eigenbrot, C. W.; Brennan, T. D.; Shusta, J.; Scheidt, W. R.; Smith, K. M. *Inorg. Chem.* **1993**, *32*, 3134-3142.
20 Song, X.-Z.; Jaquinod, L.; Jentzen, W.; Nurco, D. J.; Jia, S.-L.; Khoury, R. G.; Ma, J. G.; Medforth, C. J.; Smith, K. M.; Shelnutt, J. A. *Inorg. Chem.* **1998**, *37*, 2009-2019.
21 Scheidt, W. R.; Brancato-Buentello, K. E.; Song. H.; Reddy, K. V.; Cheng, B. *Inorg. Chem.* **1996**, *35*, 7500-7507.
22 (a) Shelnutt, J. L. In *The Porphyrin Handbook*; Kadish, K. M.; Smith, K. M.; Guilard, R., Eds.; Academic Press, San Diego, 2000, Vol. 7, pp 167-233; (b) Jentzen, W.; Ma, J. G.; Shelnutt, J. A. *Biophys. J.*, **1998**, *74*, 753-763.
23 Cullen, D. L.; Meyer Jr., E. F. *J. Am. Chem. Soc.* **1974**, *96*, 2095-2102; Gallucci, J.; Swepston, P. N.; Ibers, J. A. *Acta Cryst.* **1992**, **B38**, 2134-2139.
24 Hope, H. *Prog. Inorg. Chem.* **1994**, *41*, 1-19.
25 Sheldrick, G. M. *Acta Cryst.* **2008**, *A64*, 112-122.
26 Zhou, Y.; Wang, B.; Zhu, M.; Hou, J. G. *Chem. Phys. Lett.* **2005**, *403*, 140-145.
27 Wang, M.; Wudl, F. *J. Mater. Chem.* **2012**, *22*, 24297-24314.